# BEAT IT! HANDLING OBI IN RFOG SYSTEMS

Ayham Al-Banna, Larry Spaete, Amarildo Vieira, Sebnem ZorluOzer, Marcel Schemmann, Tom Cloonan, Dean Stoneback, Venk Mutalik
ARRIS Group, Inc.

*Abstract*

*This article investigates the OBI phenomenon in RFoG systems. Laser behavior leading to OBI events is theoretically described and laboratory experiments to investigate its effect are performed. The results show that RFoG OBI can occur prevailingly and involve more than 90% of the RFoG ONU population. Results also reveal that the preamble of DOCSIS signals is robust to the RFoG OBI problem. The concept of OBI pairs and groups is introduced to offer error-free operation. Finally, potential solutions to the OBI problem are described, which clearly demonstrate that any single-wavelength OBI-free solution for thermally-uncontrolled RFoG system must involve the CMTS support.*

## 1. INTRODUCTION

The RF over Glass (RFoG) technology offers Hybrid Fiber Coaxial (HFC) networks with high capacity potential and extends their life deep into the 2020 decade. MSOs are rapidly rediscovering that RFoG provides a cost-effective means of extending fiber all the way to the customers' premises since it employs the same infrastructure presently used in HFC systems. This technology supports fiber access as a passive optical extension of the same amplitude-modulated (AM) based optical transmission techniques that have been used in conventional HFC architectures.

The evolution of DOCSIS can help RFoG systems thorough the increased capacity offered by newly-created standards such as DOCSIS 3.1. Some of the DOCSIS 3.1 features that help increase the offered capacity include expanded spectrum support, higher order modulations, OFDM, and LDPC.

While RFoG has high potential of offering increased capacities, there are some challenges introduced by the RFoG technology that can limit the overall system performance. One of key challenges that are commonly found in RFoG systems is Optical Beat Interference (OBI). OBI is a signal degradation that occurs when two or more optical transmitters with closely spaced optical wavelengths transmit simultaneously. When two optical sources at wavelengths corresponding to optical frequencies $\omega_{o1}$ and $\omega_{o2}$ are combined at a detector, a detector output signal is produced around a center frequency ($\omega_{o1}$- $\omega_{o2}$). OBI occurs when the frequency of this noise signal overlaps with other desired RF signals' frequency range, which in turn degrades the signal-to-noise ratio (SNR) of these signals.

This paper is focused on analyzing the RFoG OBI phenomenon and its effect on network performance. This article is organized as follows: section 2 provides a general overview for the RFoG OBI signal. Section 3 introduces the calculation of the Signal-to-Interference Ratio (SIR) for RFoG systems. Wavelength drifting and broadening topics are discussed in sections 4-6. Preamble robustness to RFoG OBI is investigated in section 7. Section 8 analyzes the DOCSIS networks performance in the presence of OBI. Section 9 provides recommendations about the minimum wavelength separation to avoid OBI. OBI avoidance and mitigation is discussed in section 10. Section 11 discusses the interactions between the some of the DOCSIS 3.1 features and RFoG OBI. The article is concluded in section 12.

## 2. WHAT IS RFOG OBI?

When the fields of two optical transmitters are combined at a non-linear device, such as an optical photodetector, the total optical intensity can be expressed as [1] [2]

$$I(t) = I_1(t) + I_2(t) + I_B(t), \quad (1)$$

$$I_B(t) = 2\sqrt{I_1(t)\cdot I_2(t)}\cdot\cos\left[\left(\omega_{o1}-\omega_{o2}\right)t + \left(\phi_1(t)-\phi_2(t)\right)\right]\cdot\cos\left(\theta_{12}\right), \quad (2)$$

Where:

$I_1$ and $I_2$ are the intensities of the two optical fields,

$\omega_{o1}$ and $\omega_{o2}$ are the frequencies of the two optical signals,

$\phi_1$ and $\phi_2$ are the phases of the two optical signals,

$\theta_{12}$ is the polarization angle difference between the two optical signals,

$I_B$: beat intensity term due to the square-law nature of the photodetection process.

Observe from equation (2) that the OBI intensity depends on the relative polarization angle of the two beating signals. Parallel polarization is assumed for the analysis of this paper to yield a worst case scenario, where maximum OBI intensity is introduced due to polarization although actual real-world OBI intensities due to polarization are statistically lower. Equation (2) also indicates that the intensity of the OBI signal, which can potentially degrade the quality of US channels, depends on the wavelength (or optical frequency) separation of the beating signals. The optical spectrum of the OBI signal is the convolution of the individual optical field spectra.

Figure 1 shows an illustration of the OBI impact on the upstream RF spectrum assuming an optical field linewidth with Gaussian distribution. The optical beat power spectral density can, depending on the laser linewidth and wavelength spacing, produce low Signal-to-Interference Ratio (SIR) values meaning degraded upstream performance.

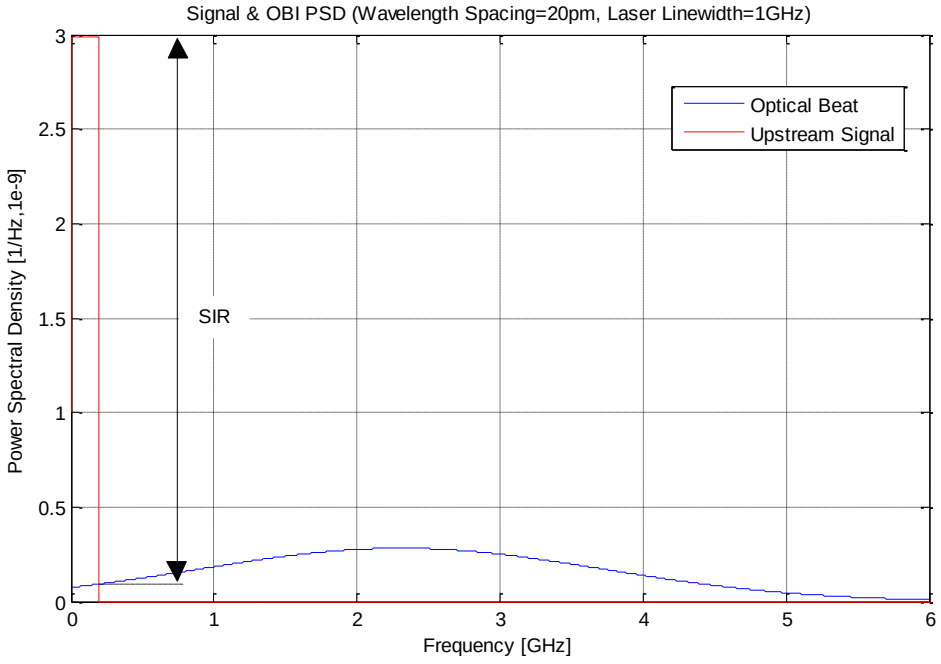


Figure 1. Upstream signal and OBI power spectrum density for 1GHz laser linewidth and 20 pm wavelength spacing

## 3. SIR CALCULATION IN RFOG SYSTEMS

The calculation of SIR for a desired optical signal in presence of an adjacent optical carrier is introduced in this section. The beat between two optical carriers at the photodetector produces a power spectrum that could be treated as interference to the desired optical signals. The power spectral density of this interference signal depends on the spectrum of the optical carriers and their frequency separation. The resultant SIR is determined by the following equation

$$SIR = 10 \cdot Log\left[\frac{\frac{1}{2}\left\langle m_i(t)^2 \right\rangle}{F(\delta f)\cdot B}\right], \qquad (3)$$

Where:

$\langle m_i(t) \rangle$ represents the detected average signal power (i.e., optical modulation index per channel),

$\delta f$ is the optical frequency difference of the two sources,

$B$ is the signal bandwidth (after roll-off).

$F(\delta f)$ represents the optical power spectrum of the interference, resulting from the convolution of the two optical fields, as a function of the optical frequency difference ($\delta f$). In order to estimate the SIR for the system, the shape of interference optical spectrum, $F(\delta f)$, needs to be specified as well. Therefore, a Gaussian linewidth assumption is made here to represent the modulated laser including the laser chirp during turn on. In this case, $F(\delta f)$ can be expressed, using Gaussian approximation, as

$$F(\delta f) = \frac{13.33}{2 \cdot \Delta f \cdot \sqrt{\pi}} \exp\left[-\left(\frac{2 \cdot \delta f}{1.2 \cdot \Delta f}\right)^2\right], \qquad (4)$$

where $\Delta f$ is the spectral width of the optical beat spectrum, which is equal to the convolution of the spectra of the two optical sources.

Calculating the SIR value can be further clarified via an example. For instance, consider 17.5% Optical Modulation Index (OMI) per channel, 5.12 MHz signal bandwidth, and 8 GHz laser linewidth operating at 1610 nm wavelength range. Figure 2 shows the SIR calculation as a function of the wavelength spacing. Observe that a minimum wavelength separation of 165 pm would be necessary in order to keep SIR above 44 dB. Note that an optical SIR of 44 dB is large enough to deliver high system SNR values that take the system RF noise into consideration. The delivered SNR values can be as large as 43 dB, which is just enough to support 4K QAM modulation supported by DOCSIS 3.1 [5]. Observe that any wavelength separation less than 165 pm will result in reduced SIR and therefore reduced system SNR values which will not be enough to support 4K QAM modulation. To show the effect of OBI on RF signals, where reduced SNR values are obtained, Fig. 3 is provided below, In particular, Fig. 3A shows high SNR values for two bonded US channels with 60% utilization where two wavelengths, separated nominally by 200 pm, are transmitting simultaneously. On the other hand, Fig. 3B shows lower SNR values due to the OBI resulting from reducing the nominal wavelength separation to 100 pm.

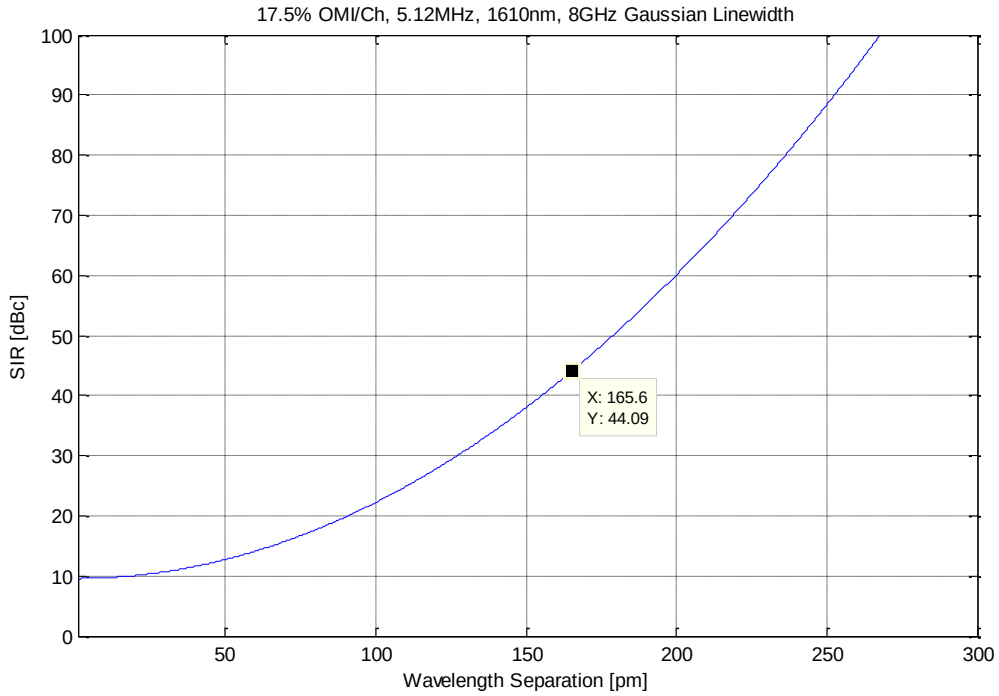


Figure 2. SIR as a function of the wavelength separation for 8GHz Gaussian linewidth

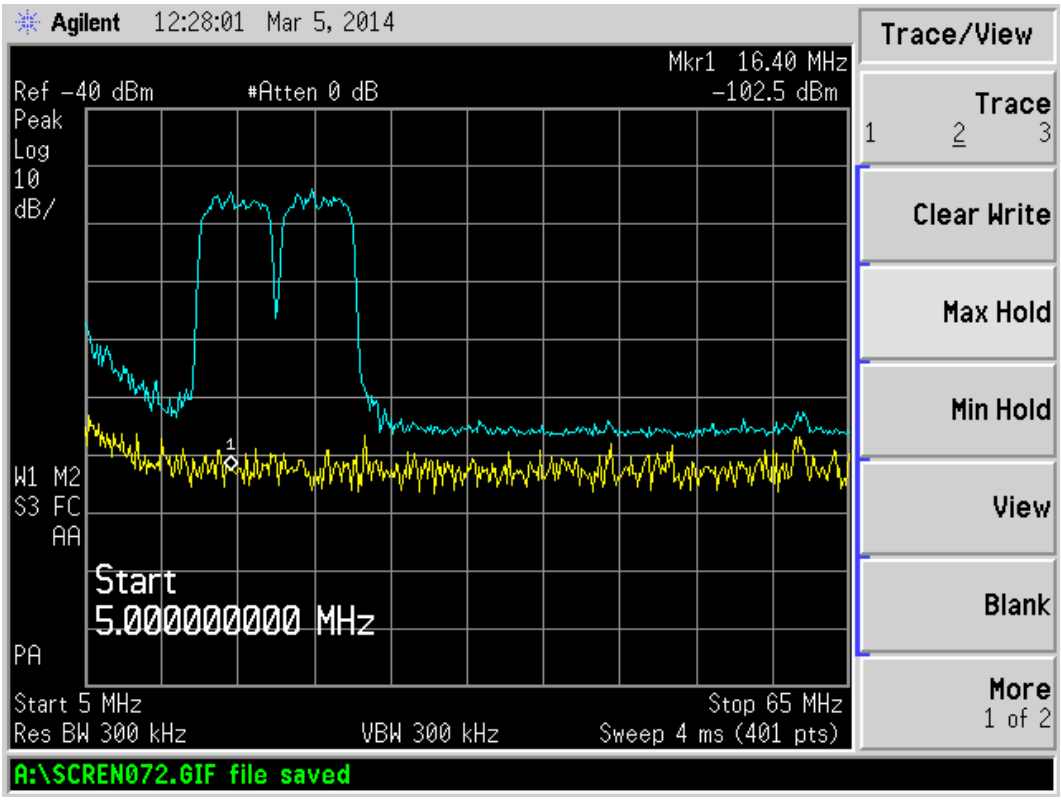


Figure 3A. High SNR values for 2 bonded US channels with wavelength separation of 200 pm

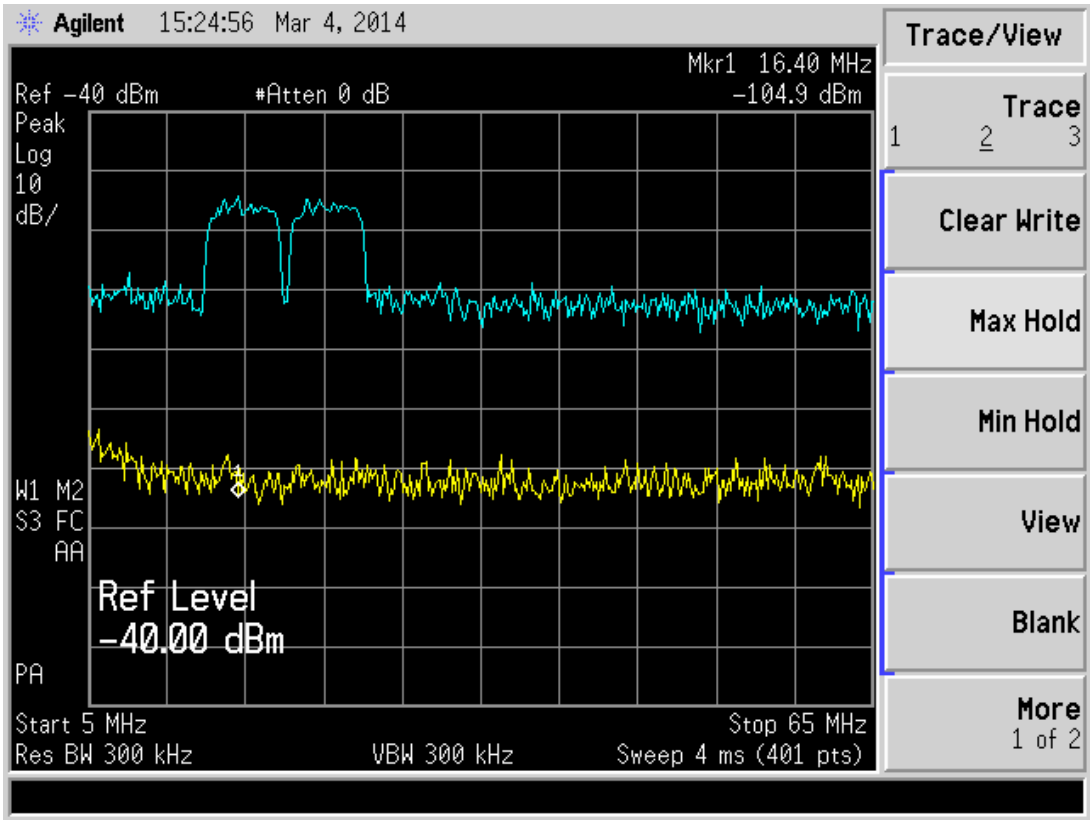


Figure 3B. Low SNR values for 2 bonded US channels with wavelength separation of 100 pm

Note that preliminary RFoG system analyses underestimated the minimum wavelength separation necessary to reduce the SIR impact on the RFoG upstream performance. Numbers between 20pm and 100pm were commonly referred to not too long ago [4], which are less than the actual required wavelength separation of at least 165 pm as shown in Fig. 2. The main issue with previous analyses was not taking in consideration two chirp factors, namely the fast wavelength broadening during the laser turn on and the thermal wavelength drift and modulation-induced wavelength broadening that occurs after the laser turns on. The next section provides in-depth analysis of wavelength drift, broadening, and separation as they are key points for understanding the OBI impact on RFoG systems, which will show that wavelength separation as large as 165 pm may not be sufficient to avoid OBI.

## 4. FAST WAVELENGTH BROADENING DUE TO LASER TURN-ON

Laser 'turn-on' causing spectral broadening, which is manifested in optical frequency oscillations around the nominal optical frequency, is well known from binary communication systems. The amount of laser chirp or drift in terms of optical frequency variations during the turn-on process can readily exceed the amount of laser chirp that occurs during modulation. It is well recognized that oscillations during the modulation cycle can be reduced if steps are taken to prevent complete turn-off of the lasers during a modulation cycle. This turn-on related laser chirp normally occurs on the sub-nanosecond timescale as photon and electron concentrations in the laser need to balance as laser turns on. However, the situation is different in RFoG systems from such binary

systems! Firstly, the relevant time scales of laser turn on/off are much longer (microseconds to milliseconds), secondly, the lasers must be turned off completely in RFoG systems such that the output power in the off state cannot cause OBI with other sources in the system. Whereas the linewidth broadening (i.e., optical frequency variations) due to chirp induced by modulation and laser turn-on is relatively small in RFoG systems, the thermally-induced chirp is large, which can be more than an order of magnitude larger as will be shown later.

## 5. WAVELENGTH DRIFT DUE TO THERMAL PROCESSES & BROADENING DUE TO MODULATION

Thermally induced chirp is important for processes with slow time constants [3], which are typically longer than 100 nsec. Thermal processes cause wavelength drifting from the nominal wavelength value due to laser heating and cooling during and between transmission bursts. It will be shown later in this section than the laser wavelength drift is fast for the first few microseconds and then slows down after that.

The laser response time to modulation is instantaneous and therefore the laser wavelength oscillates around the drifted wavelength value causing spectral broadening due to modulation. This section discusses the thermally induced wavelength drift and its consequences for data errors caused by OBI.

The ONU in RFoG systems is operated in a burst mode and therefore it is off most of the time on average, which allows the laser to cool during that time. When a burst needs to be transmitted the laser is turned on and heat is dissipated. The semiconductor laser generally has a narrow stripe (width on the order of a few micrometers) that is used to confine light in a single mode so that it can be coupled efficiently to the fiber. Most of the dissipation (series resistance and optical absorption losses) take place in the stripe area. Due to the relevant dimensions of this area and the semiconductor material properties, the thermal response time constant of the laser stripe is in the range of few 100 nanoseconds to microseconds, which is on the order of the length of the preamble of DOCSIS bursts.

The heat generated in the stripe area then needs to be transferred from the laser crystal through solder joints to the heat-sink, which takes place on significantly slower time scales on the order of the duration of the burst transmission and even longer. A quick example is provided below to appreciate the scale of contributions of modulation induced chirp and thermally induced chirp. In this example, assume a typical laser with forward voltage ($V_{bias}$) of 1.2V that is operated at a current ($I_{bias}$) of 40 mA, which is mostly dissipated as $P_{diss}$ (48mW) apart from a small amount of produced optical power. Additionally, assume a thermal resistance of $R_{th}$ 90 K/W. This yields a heat-up (dT) of just over 4 Kelvin resulting in a thermal drift $d\lambda$ of up to 0.35 nm (or 346 pm) as calculated below. Note that the thermal drift calculated here (346 pm) is larger than the SIR-based estimation for wavelength separation performed earlier (165 pm) because the analysis in this section takes the temperature variations into consideration.

$$dT := R_{th} \cdot \frac{P_{diss}}{1000} \qquad dT = 4.32 \quad K$$

$$d\lambda_{dT} := 0.08 \quad \text{nm per K}$$

$$d\lambda := d\lambda_{dT} \cdot dT \qquad d\lambda = 0.346 \quad \text{nm} \qquad . \quad (5)$$

Given an example effective modulation index ($\mu$) of 0.22, a threshold current ($I_{th}$) of 6 mA, and a laser Frequency Modulation FM response to electrical modulation (FM) of 120

MHz/mA, the modulation induced chirp (or spectral broadening) can be calculated as

$\mu := 0.22$ Effective modulation index

$FM := 120$ MHz per mA modulation response

$df := (I_{bias} - I_{th}) \cdot \mu \cdot FM$ MHz laser chirp due to modulation $df \cdot 10^{-3} = 0.898$ GHz . (6)

Even for higher chirp lasers, the laser chirp (or modulation-induced spectral broadening) translates to less than 20 pm of width for the modulated laser spectrum. This value is relevant for OBI likelihood of occurrence in the sense that when two lasers are transmitting at wavelengths separated by 20 pm or less, then their modulated spectra partially overlap and severe OBI can occur. Note that the above analysis only applies if no wavelength drifting is present.

However, in the real world, spectral broadening is superimposed on the thermal drift to form the instantaneous laser wavelength value. Since it was shown earlier that the potential thermal drift can be up to 346 pm and the spectral widening (or chirp) is about 20 pm, then the total is about 400 pm. Therefore, it will be safe to assume that wavelength separation of at least 500 pm is necessary to guarantee that OBI does not occur.

## 6. CHARACTERIZING THE THERMAL LASER WAVELENGTH DRIFT

To investigate the thermal laser wavelength drift, a laboratory experiment was performed, where a 1310 nm Distributed Feedback (DFB) laser was operated at 10% duty cycle to simulate an ONU in a high usage case as shown in Fig. 4. In this experiment, the laser is not producing light during the burst time except for very short amount of time when the wavelength measurements are performed. In particular, the laser was biased just under threshold to induce 6 mW of dissipation during bursts (i.e., not emitting light), while it was off between bursts (0mW). For a small fraction of time within the burst (i.e., <0.5% of burst time, 0.05% overall duty cycle), the laser was putting out light by being biased to just above threshold to induce 13.5 mW of dissipation. Observe that this is insignificant compared to the overall dissipation during the burst.

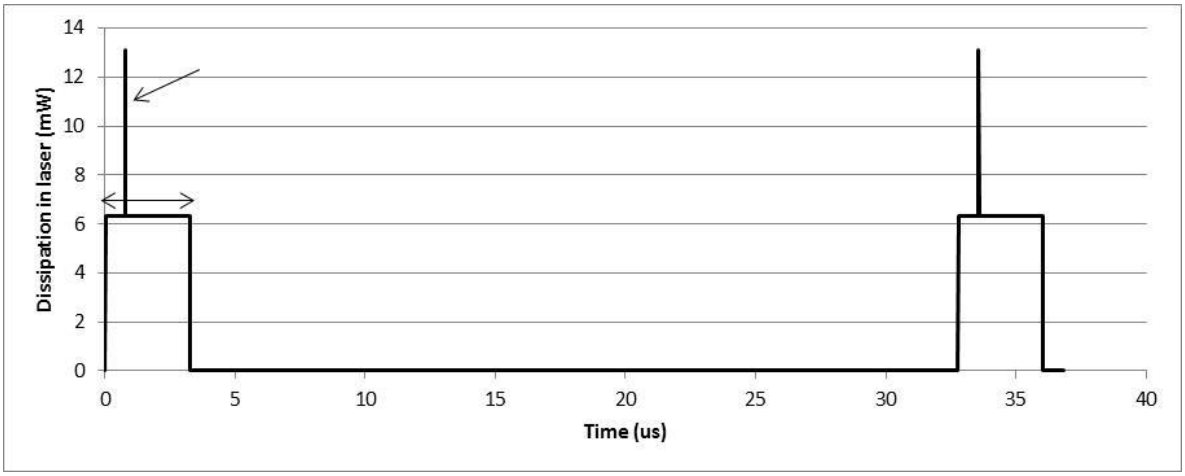


Figure 4. Laser operated with duty cycle of 10% to simulate highly-utilized ONU

Observe that the laser is off most of the time (0 mW), while during the bursts, the laser is turned on just below threshold such that power is dissipated in the device. In this case, the laser is technically not emitting light and therefore optical output power is negligible during this time except for a brief pulse (narrow spike in Fig. 4) that drives the laser just above threshold and therefore emitting light. Wavelength measurements are then performed using a spectrum analyzer.

The wavelength drift due to thermal processes was investigated by changing the location of the pulse throughout the burst duration (horizontal arrow on Fig. 4). In particular, since the wavelength of the DFB laser is linearly related to the cavity temperature, the procedure of shifting the pulse provides a "sample" of the cavity temperature at various times throughout the burst. Figure 5 shows the observed wavelength drift during the burst due to thermal processes, where wavelength measurements occurred over duration of about 200 usec.

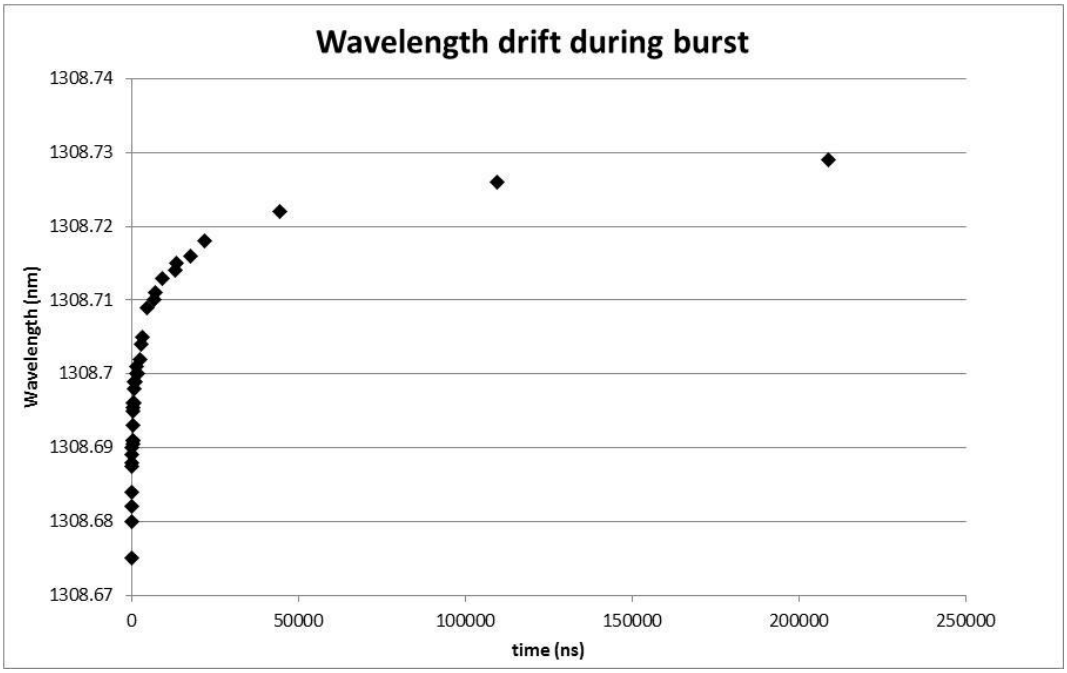


Figure 5. Wavelength drift during bursts

Observe that Fig. 5 captures wavelength drift in the 10 ns-200 usec range, where most of the wavelength drift occurs early in the burst. The curve in Fig. 5 is scaled to reflect operation at 40 mA and plotted on a logarithmic x-axis as shown in Fig. 6.

Again, it can be observed from Fig. 6 that most of the wavelength drift occurs in the first microseconds of the burst time as the laser is heating up. However, slower time constants take over as time progresses and the wavelength continues to drift slowly throughout the burst.

This implies that the probability of an OBI event during the preamble of the transmitting laser is high. However, the duration of such an OBI event is generally short as can be observed from the curve shown in Fig. 7. This curve which shows the duration of an OBI event to cross $\pm$20pm wavelength region at different instant of times during the burst (based on wavelength drift rate at those time instants, which can be calculated from Fig. 6).

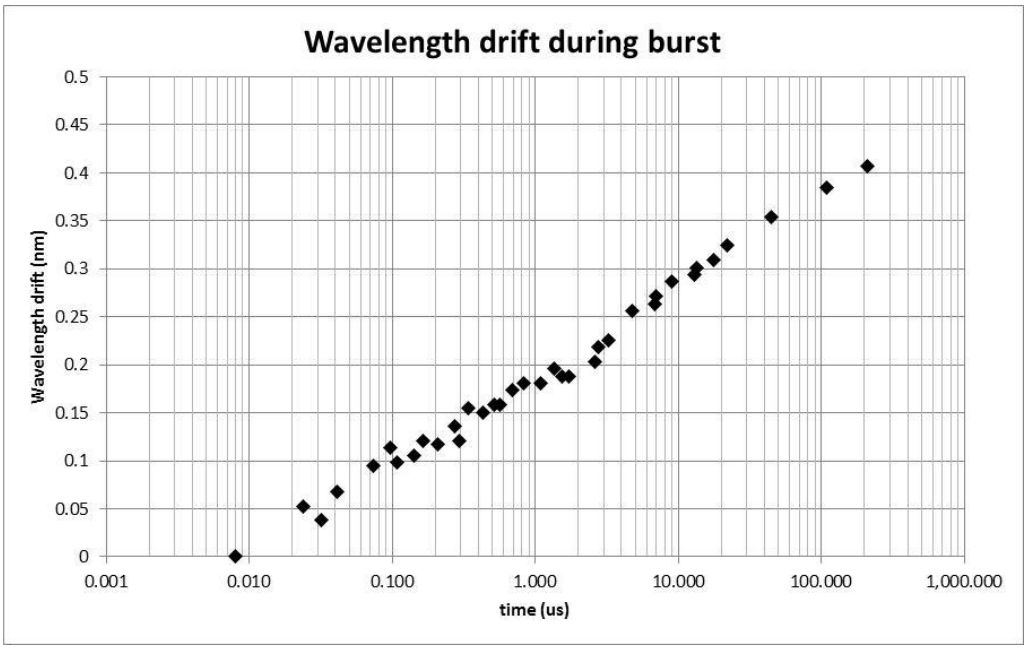


Figure 6. Scaled wavelength drift during bursts (at 40mA bias current) and plotted on logarithmic x-axis

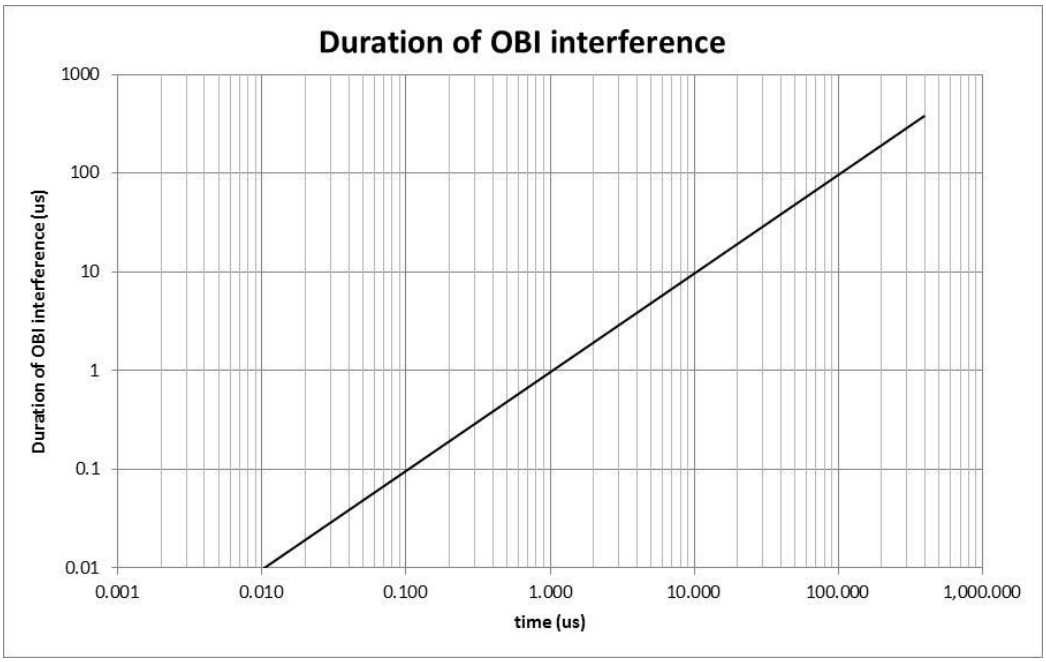


Figure 7. Estimating the duration of OBI events (US interference) throughout the burst time

The next section will describe extensive experiments that were performed to investigate the robustness of the preamble signal to OBI. Those experiments will show that the preamble can survive even in the presence of severe OBI. Observe that for longer time scales into the burst (e.g., 100 usec into a burst), the change rate becomes so slow that OBI events can last more than 100 usec and cause uncorrectable error bursts.

## 7. ROBUSTNESS OF DOCSIS PREAMBLE TO RFOG OBI

It is important to realize that US packets can be lost due to data and/or preamble corruption. In particular, if US noise or collisions (due to OBI or other reasons) cause significant number of errors in the data portion of the US transmission, then FEC may not be able to recover all of the damaged bits which in turn yields to one or more corrupted codewords (CWs). Lost CWs lead to dropped packets! In the case when excessive noise or collisions corrupt the preamble of an US burst, the receiver may not be able to identify the burst and therefore all data bits carried in that burst will be lost.

The previous sections described the laser wavelength drift that occurs as the laser turns on for transmission. The fast drift in the wavelength occurs over the first few microseconds of the transmission. In general, as the laser heats up for transmission, the wavelength changes by about 200pm over the few microseconds, which will likely cause multiple collisions between the current transmission and other ongoing transmissions. While these collisions can affect ongoing transmissions anywhere in the transmission (i.e., beginning, middle, or end of transmissions), they will affect the current transmission solely during the preamble.

FEC is normally used to protect the data portion of US transmissions from noise. Therefore some errors caused by these short duration collisions can be recovered. On the other hand, the effect of multiple collisions on the preamble is unknown. As a result, an emulation laboratory experiment was designed and performed to investigate the robustness of the preamble of DOCSIS signals to collisions caused by the RFoG OBI phenomenon. This emulation experiment was performed with a cable-only network to control the test environment. The obtained results were validated with an RFoG lab experiment, where real OBI event occurred over fiber links.

In this experiment, the RFoG OBI events were emulated as short-duration wideband impulse noise. The impulse noise was generated with an external signal generator and added to US bursts. Three different impulse noise patterns were generated:

1. Two short-duration impulses (1 usec) with 10 usec in between as shown in Fig. 8.
2. Two short-duration impulses (1 usec) with 30 usec in between as shown in Fig. 9.
3. One medium-duration impulse (9 usec) as shown in Fig. 10.

All of the above patterns have a nominal period of 4 msec. The amplitude(s) of the generated impulse(s) in the above patterns got adjusted such that a specific SNR value (e.g., 0 or -7.5 dB) is obtained during the short impulses. For instance, in the 0 dB SNR case, the impulse noise level was set such that it is equal to the data portion signal level.

The US traffic was transmitted over an ATDMA channel via UGS grants with a nominal period of 4 msec. Very insignificant jitter was allowed for those transmissions. The size of the UGS grant was set to 150B such that two FEC codewords (78B max size) were used to transmit a single data packet (100B each). 10,000 packets were transmitted for each experiment run. The US channel width was configured to be 6.4 MHz which yields 5.12 Msps. The preamble length was 104 bits (or 52 QPSK symbols), which in turn occupies about 10 usec. Different preamble power values (i.e., QPSK0, QPSK1) were experimented to fully characterize the preamble robustness. Observe that a QPSK0 preamble will have the same level as the data portion of the signal. On the other hand, the power of the QPSK1 preamble is 3 dB higher than the signal power.

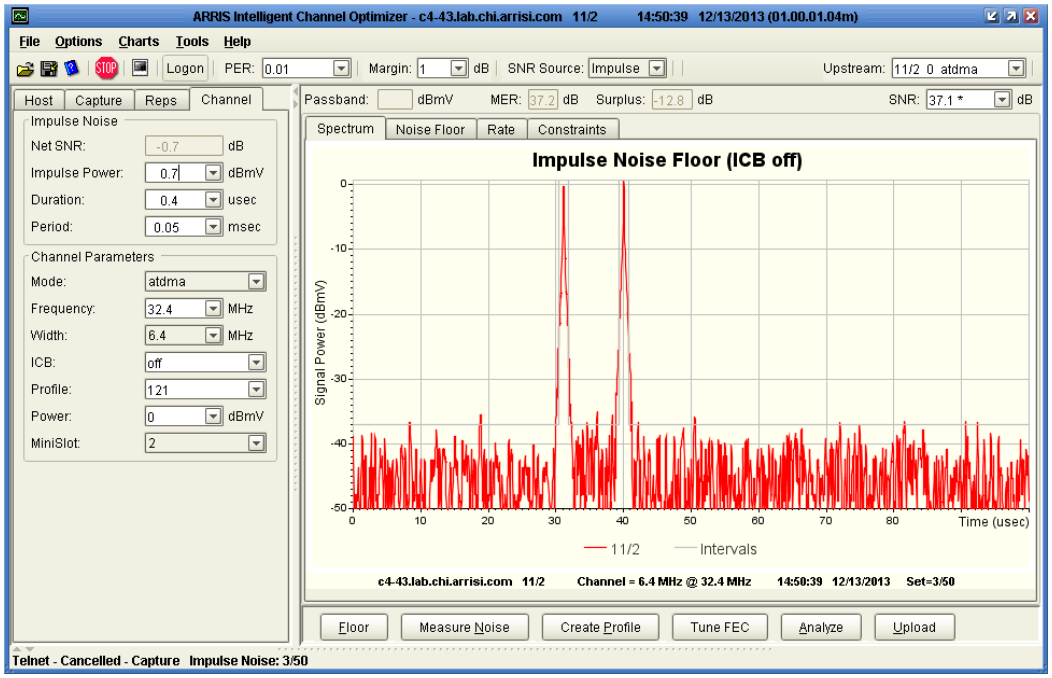


Figure 8. RFoG OBI noise pattern 1: Two short-duration impulses (1 usec) with 10 usec in between. Impulse noise level is 7.5 dBmV higher than the signal level

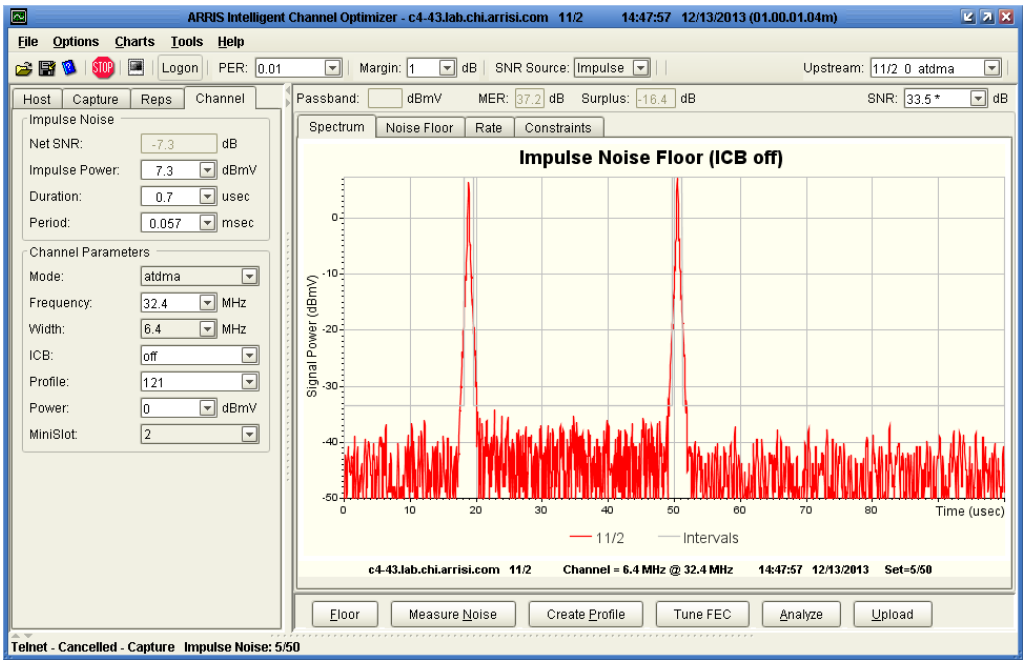


Figure 9. RFoG OBI noise pattern 2: Two short-duration impulses (1 usec) with 30 usec in between. Impulse noise level is 7.5 dBmV higher than the signal level

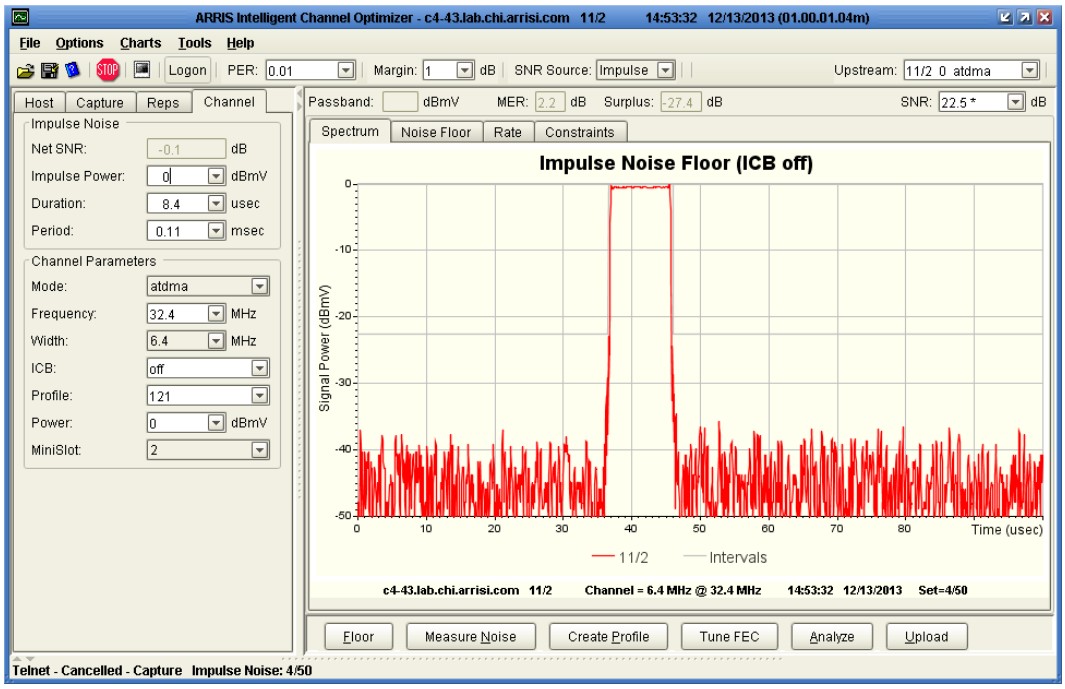

Figure 10. RFoG OBI noise pattern 3: One medium-duration impulse (9 usec). Impulse noise level is 0 dBmV (equal to the signal level)

Since the preamble in the above UGS grant is about 10usec long, the third noise pattern above (impulse width of 9usec) was considered to be the worst case scenario where the majority of the preamble is damaged by an RFoG OBI event (if synchronized). This is not likely to happen in the real world, where OBI events tend to be short in duration although more than one OBI event can affect the preamble. Therefore, noise patterns 1 and 2 are more likely to emulate real-world OBI events.

While impulse noise and UGS data bursts have the same nominal period of 4 msec, the period of the impulse noise was set to a value that is slightly different than the period of the UGS bursts. The slight asynchronization between impulse noise and UGS grants resulted in a situation where the impulse appear to slide across the UGS grants on an Oscilloscope screen as shown in Figs. 11A and 11B. The sliding event on the oscilloscope screen is actually an illusion caused by the fast capture of multiple impulses damaging different (and sequential) parts of different bursts. At any instant of time, the impulse would either corrupt the preamble or the data or does not collide with the UGS signal at all. Running the traffic and noise for a sufficient period of time will yield to a situation, where impulse is corrupting different portions of the preamble of the UGS grants.

For each experiment run, the number of lost packets due to preamble damage (lost bursts) or data damage (unrecovered FEC CWs) was recorded. A summary of the results is shown in Table 1. Observe that the packet loss measurements in the table show that the preamble of DOCSIS signals is very robust to RFoG OBI events. In particular, no packets were lost due to preamble damage even with the worst case OBI noise (pattern 3)! On the other hand, some packets were lost due to OBI events corrupting data FEC codewords. The preamble robustness is also demonstrated by an RFoG lab experiment were real-world OBI events occurred but could not cause packet loss due to preamble damage.

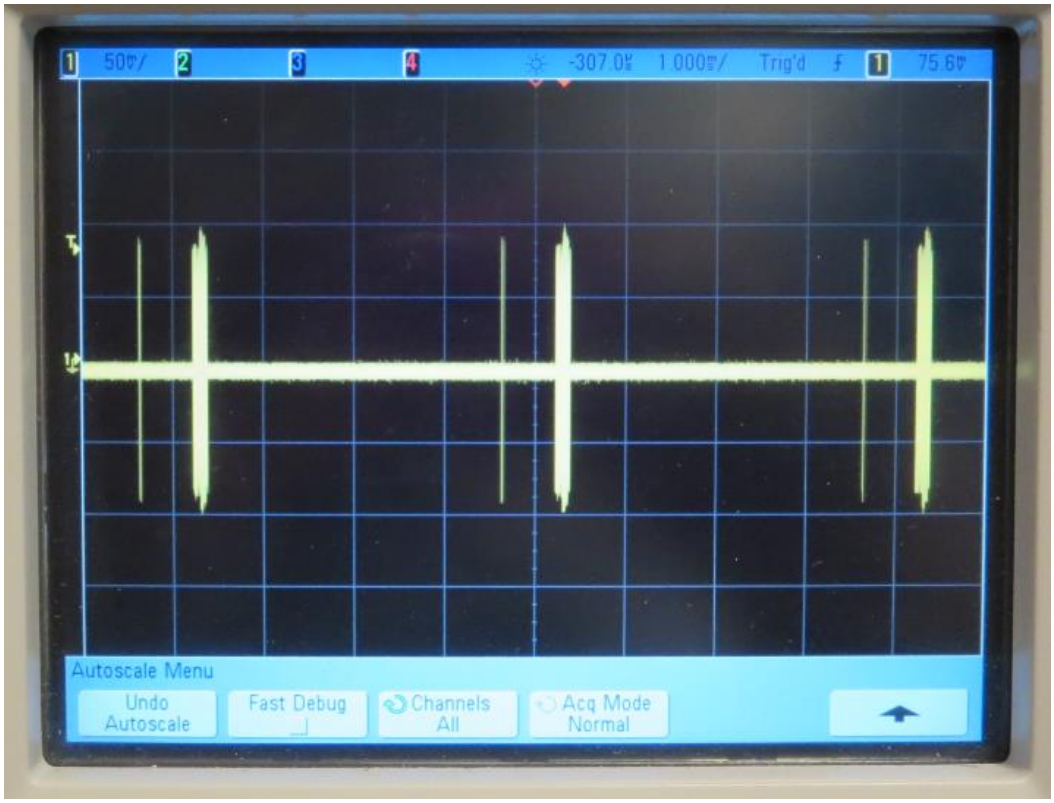


Figure 11A. Multiple impulses getting close to corrupt multiple UGS grants


Figure 11B. Multiple impulses are corrupting multiple UGS grants. Note the signal & noise addition.

Table 1. DOCSIS UGS packet loss due to preamble or data damage caused by RFoG OBI

| Test ID | UGS Preamble Type | UGS Modulation Order | RFoG OBI Pattern | SNR (dB) | Corrected FEC CWs | Packets Loss due to FEC | Packets Loss due to Preamble |
|---|---|---|---|---|---|---|---|
| 1 | QPSK0 | QPSK | 1 | 0 | 418 | 0 | 0 |
| 2 | QPSK0 | QPSK | 1 | -7.5 | 634 | 0 | 0 |
| 3 | QPSK0 | QPSK | 2 | 0 | 411 | 0 | 0 |
| 4 | QPSK0 | QPSK | 2 | -7.5 | 675 | 0 | 0 |
| 5 | QPSK0 | QAM-64 | 1 | 0 | 283 | 0 | 0 |
| 6 | QPSK0 | QAM-64 | 1 | -7.5 | 248 | 28 | 0 |
| 7 | QPSK0 | QAM-64 | 2 | 0 | 430 | 2 | 0 |
| 8 | QPSK0 | QAM-64 | 2 | -7.5 | 377 | 18 | 0 |
| 9 | QPSK1 | QPSK | 1 | 0 | 409 | 0 | 0 |
| 10 | QPSK1 | QPSK | 1 | -7.5 | 638 | 0 | 0 |
| 11 | QPSK1 | QPSK | 2 | 0 | 434 | 0 | 0 |
| 12 | QPSK1 | QPSK | 2 | -7.5 | 657 | 0 | 0 |
| 13 | QPSK1 | QAM-64 | 1 | 0 | 302 | 3 | 0 |
| 14 | QPSK1 | QAM-64 | 1 | -7.5 | 246 | 30 | 0 |
| 15 | QPSK1 | QAM-64 | 2 | 0 | 396 | 0 | 0 |
| 16 | QPSK1 | QAM-64 | 2 | -7.5 | 377 | 16 | 0 |
| 17 | QPSK0 | QPSK | 3 | 0 | 633 | 40 | 0 |
| 18 | QPSK0 | QAM-64 | 3 | 0 | 19 | 135 | 0 |
| 19 | QPSK1 | QPSK | 3 | 0 | 613 | 50 | 0 |
| 20 | QPSK1 | QAM-64 | 3 | 0 | 15 | 136 | 0 |

## 8. PEFORMANCE OF DOCSIS NETWORKS IN RFOG ARCHTECTURE

Earlier sections in this paper provided an overview of the wavelength drifts and broadening and also described the OBI problem. An empirical analysis to show the preamble robustness in the presence of simulated OBI event in a cable-only network setup was also provided. This section introduces a set of laboratory experiments over a real-world setup of fiber network to characterize the OBI phenomenon and its occurrence likelihood in a population of RFoG ONUs. These experiments are also designed to validate the theoretical analyses that were provided in previous sections to estimate the wavelength separation needed between two optical transmitters such that OBI does to not occur. The experiments described below will also verify the conclusions that were made regarding robustness of the DOCSIS preamble based on the cable-only emulation experiment described in the previous section. The performance of DOCSIS networks in the RFoG architecture is determined via these experiments. Finally, some of the OBI mitigation schemes are verified to operate and offer virtually error-free performance in RFoG networks.

This experiment setup was composed of a CMTS, 32 CMs, 32 RFoG ONUs, optical headend transmitter/receiver, and 20 km of fiber links connected as shown in Fig. 12. The nominal DS wavelength was 1550 nm and the nominal US wavelength was 1610 nm.

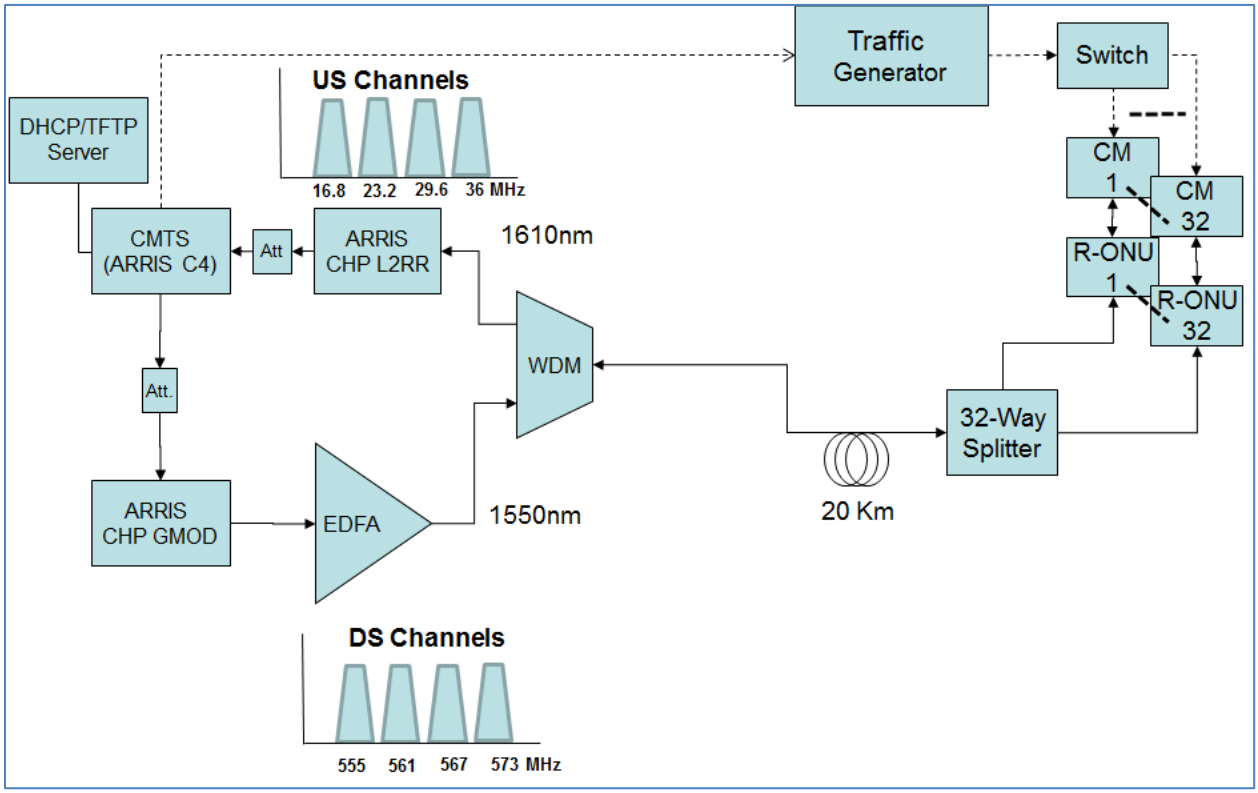


Figure 12. RFoG architecture experiment setup

The CMTS was setup with 4 6.4 MHz US channels operated at QAM64 modulation (T= 12B, CW_size = 81B for short grants, T= 16B, CW_size = 223B for long grants). The first step that was performed is to 'manually' measure the wavelengths of different ONUs using an optical wavelength meter, where the wavelength of the ONU is measured after transmitting a CW tone through the ONU. Given that the wavelength varies over time, the absolute wavelength value will represent a snapshot at a time instant and therefore may not be very definite or descriptive. However, taking wavelength measurements for all ONUs in the same fashion can provide relative wavelength relationships between the different ONUs. Two sample measurements were taken for each ONU: 1) right after the laser is turned on, 2) after 30 seconds. The collected ONUs wavelength measurements are then sorted in ascending order based on the 30 sec reading as shown in Table 2. It is commonly known that less than 20pm inter-wavelength separation is needed for OBI to occur. Therefore, this rule was used to identify the OBI pairs in the ONU population. Later in this section, our analysis will show that it will take much more than 20pm of wavelength separation for OBI not to occur.

Table 2. Wavelength measurements for ONU population

| ONU ID | λ 1st value (nm) | λ 30 Sec value (nm) | Wavelength difference based on 1st reading | Potential OBI pairs based on 1st reading | Wavelength difference based on 30 sec reading | Potential OBI pairs based on 30 sec reading |
|---|---|---|---|---|---|---|
| 15 | 1611.041 | 1611.075 | | | | |
| 31 | 1611.108 | 1611.142 | 0.067 | | 0.067 | |
| 6 | 1611.118 | 1611.157 | 0.01 | 6,31 | 0.015 | 6,31 |
| 18 | 1611.174 | 1611.204 | 0.056 | | 0.047 | |
| 12 | 1611.225 | 1611.269 | 0.051 | | 0.065 | |
| 13 | 1611.372 | 1611.395 | 0.147 | | 0.126 | |
| 4 | 1611.382 | 1611.426 | 0.01 | 4,13 | 0.031 | 4,13 |
| 23 | 1611.44 | 1611.476 | 0.058 | | 0.05 | |
| 19 | 1611.532 | 1611.563 | 0.092 | | 0.087 | |
| 30 | 1611.573 | 1611.606 | 0.041 | | 0.043 | |
| 27 | 1611.655 | 1611.694 | 0.082 | | 0.088 | |
| 3 | 1611.675 | 1611.709 | 0.02 | 3,27 | 0.015 | 3,27 |
| 14 | 1611.881 | 1611.925 | 0.206 | | 0.216 | |
| 28 | 1611.914 | 1611.949 | 0.033 | | 0.024 | |
| 32 | 1611.957 | 1611.99 | 0.043 | | 0.041 | |
| 10 | 1612.022 | 1612.052 | 0.065 | | 0.062 | |
| 2 | 1612.037 | 1612.089 | 0.015 | 2,10 | 0.037 | |
| 24 | 1612.189 | 1612.225 | 0.152 | | 0.136 | |
| 29 | 1612.199 | 1612.251 | 0.01 | 29,24 | 0.026 | |
| 21 | 1612.305 | 1612.351 | 0.106 | | 0.1 | |
| 5 | 1612.354 | 1612.386 | 0.049 | | 0.035 | |
| 11 | 1612.408 | 1612.432 | 0.054 | | 0.046 | |
| 25 | 1612.536 | 1612.57 | 0.128 | | 0.138 | |
| 9 | 1612.732 | 1612.671 | 0.196 | | 0.101 | |
| 26 | 1612.732 | 1612.763 | 0 | 9,26 | 0.092 | |
| 7 | 1613.073 | 1613.107 | 0.341 | | 0.344 | |
| 8 | 1613.107 | 1613.149 | 0.034 | | 0.042 | |
| 17 | 1613.171 | 1613.199 | 0.064 | | 0.05 | |
| 20 | 1613.293 | 1613.33 | 0.122 | | 0.131 | |
| 1 | 1613.403 | 1613.43 | 0.11 | | 0.1 | |
| 16 | 1613.857 | 1613.888 | 0.454 | | 0.458 | |
| 22 | 1614.175 | 1614.203 | 0.318 | | 0.315 | |

The next step was running some baseline experiments. The first experiment had all CMs placed on a single US channel and ran US traffic through all CMs and obtained an error free operation. Afterwards, a second US channel was enabled and all modems were configured to be able to bond across both US channels. US traffic source was configured to achieve about 70% US channel utilization with 218 B packets. To achieve 70%

utilization, each CM was bursting at 1.14Mbps (assuming 26Mbps US channel capacity after DOCSIS overhead is removed). US traffic was run for 5 minutes and the traffic source counts as well as the CMTS FEC counts were monitored after the transmission of the US traffic had completed. The error counts showed that all CMs experienced FEC errors and most CMs had dropped more than 1% of the packets. The results showed packet loss values in the range of 0.01% - 4.99% with uncorrectable FEC codeword rates in the range of 0.01% - 4.19%. Another baseline experiment was performed with 4 bonded US channels with 70% US channel utilization. More OBI occurred between CMs and the results showed that packet loss rates increased to the 8.38% - 25.11% range. In this experiment, the uncorrected FEC codeword rates also increased and fell in the 7.18% - 22.59% range. It is obvious that increasing the number of bonded US channels increases the likelihood of OBI occurrence.

Further experiments were performed, where US traffic is run through CMs and CMTS FEC counts were monitored to identify the exact OBI pairs in the ONU population. The summary of the pairs is provided in Table 3. Note that the data for OBI partners in Table 3 is based on strong OBI relationship between partners. That is, simultaneous transmissions from partners yield significant OBI that causes large amount of FEC errors. Minor (less damaging) OBI can result from simultaneous transmissions from some non-partners. Minor OBI partners can also be included but these minor OBI partners will lead to relationships that tie almost all CMs to each other and it will be difficult to cleanly separate the population into solid partners.

Observe that any attempt to relate the above relationships (partners) to the wavelength measured earlier (in Table 2) using the 20pm rule, results in missing many of the pairs. Therefore, the 20pm rule does not offer high potential for identification of the OBI candidates. Some of the partners in Table 3 are common for different ONUs and therefore the next step was to sort the partners into groups such that simultaneous transmissions of members that belong to the same group will result in damaging OBI. The groups are shown in Table 4 and these groups are independent (ignoring minor OBI relationships), which means that simultaneous transmissions from members of different groups will not produce damaging OBI. Note that Group # 5 represents the group of members that have no OBI partners.

Based on the above grouping, an analysis was performed on the wavelength measurements in Table 2 to relate groups to wavelengths as shown in Table 5.

Note that, in theory, the members of each of the groups above can OBI with each other while members of different groups do not OBI with each other. Therefore, groups could be intelligently assigned to US channels. In this experiment were only 2 US channels are enabled, error-free operation was achieved when groups 0, 1, 3 were assigned to US0 (total of 16 CMs) and groups 2, 4, 5 were assigned to US1 (total of 16 CMs). Observe that members of group 5 (non-OBI candidates) could have been assigned to bond across both channels. Two different 5-minute US traffic runs (37% and 88% channel utilization) were performed and both resulted in zero FEC errors for all CMs.

Table 3. OBI partners for to each ONU

| ONU ID | OBI Partner(s) |
|---|---|
| 1 | 20 |
| 2 | 32, 10 |
| 3 | 27, 30 |
| 4 | 12, 13, 6, 18, 23 |
| 5 | 21, 11 |
| 6 | 15, 18, 31 |
| 7 | 8 |
| 8 | 7, 17 |
| 9 | 26 |
| 10 | 2, 32 |
| 11 | 5, 25 |
| 12 | 4, 6, 18 |
| 13 | 4, 12 |
| 14 | 28 |
| 15 | 6, 31 |
| 16 | No partner |
| 17 | 8, 20 |
| 18 | 6, 31, 12, 4 |
| 19 | 27, 30, 23 |
| 20 | 1, 17 |
| 21 | 5, 29 |
| 22 | No partner |
| 23 | 4, 30, 19 |
| 24 | 29 |
| 25 | 11 |
| 26 | 9 |
| 27 | 3, 19, 30 |
| 28 | 14, 32 |
| 29 | 21, 24 |
| 30 | 3, 27, 19, 23 |
| 31 | 6, 15, 18 |
| 32 | 2, 10 |

Table 4. OBI partners in Table 3 are sorted into groups

| Group ID | Group Members | Number of Members |
|---|---|---|
| 0 | 1, 7, 8, 17, 20 | 5 |
| 1 | 2, 10, 14, 28, 32 | 5 |
| 2 | 3, 4, 6, 12, 13, 15, 18, 19, 23, 27, 30, 31 | 12 |
| 3 | 5, 11, 21, 24, 25, 29 | 6 |
| 4 | 9, 26 | 2 |
| 5 | 16, 22 | 2 |

Table 5. Relationship between wavelength measurements & groups (based on Table 2)

| ONU ID | λ 30 Sec value (nm) | Wavelength difference based on 30 sec reading | Potential OBI pairs based on 30 sec reading | Group ID |
|---|---|---|---|---|
| 15 | 1611.075 | | | 2 |
| 31 | 1611.142 | 0.067 | | |
| 6 | 1611.157 | 0.015 | 6,31 | |
| 18 | 1611.204 | 0.047 | | |
| 12 | 1611.269 | 0.065 | | |
| 13 | 1611.395 | 0.126 | | |
| 4 | 1611.426 | 0.031 | 4,13 | |
| 23 | 1611.476 | 0.05 | | |
| 19 | 1611.563 | 0.087 | | |
| 30 | 1611.606 | 0.043 | | |
| 27 | 1611.694 | 0.088 | | |
| 3 | 1611.709 | 0.015 | 3,27 | |
| 14 | 1611.925 | 0.216 | | 1 |
| 28 | 1611.949 | 0.024 | | |
| 32 | 1611.99 | 0.041 | | |
| 10 | 1612.052 | 0.062 | | |
| 2 | 1612.089 | 0.037 | | |
| 24 | 1612.225 | 0.136 | | 3 |
| 29 | 1612.251 | 0.026 | | |
| 21 | 1612.351 | 0.1 | | |
| 5 | 1612.386 | 0.035 | | |
| 11 | 1612.432 | 0.046 | | |
| 25 | 1612.57 | 0.138 | | |
| 9 | 1612.671 | 0.101 | | 4 |
| 26 | 1612.763 | 0.092 | | |
| 7 | 1613.107 | 0.344 | | 0 |
| 8 | 1613.149 | 0.042 | | |
| 17 | 1613.199 | 0.05 | | |
| 20 | 1613.33 | 0.131 | | |
| 1 | 1613.43 | 0.1 | | |
| 16 | 1613.888 | 0.458 | | 5 |
| 22 | 1614.203 | 0.315 | | |

The above approach was verified with 4 US channels, where groups 0, 4 were assigned to US0, groups 1 &5 were assigned to US1, group 2 was assigned to US2, group 3 was assigned to US3 and ran with 70% channel utilization. The results after 5 minutes run were virtually error free (max of $1.27x10^{-5}$ or 0.001% of uncorrectable FEC).

Another experiment was performed where UGS flows were setup to test the preamble robustness to verify the results obtained by the cable-only emulation experiment. UGS flows were transmitted via all CMs which were bonded on 2 US channels. OBI incurred caused some loss in DATA packets but no bursts were lost due to preamble damage.

Observe that the above experiments were performed with a single packet size of 218B based on packet size statistics that were collected recently. To obtain a controlled environment, the experiments were run with fixed packet rate across all CMs to obtain certain US channel utilization. In reality, various services (e.g., voice, data) are offered over an RFoG architecture, where these services have with different on-off times and packet distributions. These characteristics can affect the way the US utilization and will also impact the likelihood of OBI occurrence. Additionally, various applications have different packet loss, delay, and jitter requirements.

In conclusion for this experiment, it can be noted that from the above experiments that OBI is a prevalent problem that can affect most of the populations. In particular, 30 out of 32 ONUs had OBI partners. While the preamble of DOCSIS signals is robust to RFoG OBI, OBI can cause data damage and corresponding packet loss. Once the OBI pairs or partners were identified, the OBI partner groups were intelligently assigned to US channels to offer virtually error-free operations with multiple channels, where members of each OBI partner group are confined to a single US channels. The CMTS scheduler could be augmented to not limit a group of partners to a single group. In particular, the CMTS can offer an error-free operation in an RFoG environment as long as it scheduled simultaneous transmissions from members of different groups. In a nut shell, CMTS configuration and CMTS scheduler augmentation must be involved in any single nominal wavelength solution to offer an error-free operation in a thermally-uncontrolled RFoG environment.

## 9. WAVELENGTH SEPARATION NEEDED FOR OBI AVOIDANCE

Earlier in section 5 of this paper, theoretical analyses showed that a minimum requirement of 500 pm of wavelength separation is necessary for OBI not to occur at all. Additionally, analysis is performed in this section to show that wavelength separation values less than 200 pm will result in significant OBI occurrence leading to large amounts of packet loss. In particular, more experiments based on the setup shown in Fig. 12 were performed and a Monte Carlo MATLAB simulation was implemented based on the experimental 30-sec wavelength measurements provided earlier in Table 2. Those wavelength measurements were assigned to the simulated ONUs to estimate the amount of OBI that occurs in the system. In practice, wavelengths continuously change due to drift and broadening as described earlier, therefore, the simulation can be viewed as a snap shot of time with fixed wavelength values.

The MATLAB model is a Monte Carlo tool used to estimate the impact of OBI on data loss based on the wavelength spacing among the ONUs, when two or more ONUs are transmitting at the same time. No FEC correction is assumed in the model. When an OBI event occurs between two ONUs, it is assumed that all channels are corrupted and

therefore data from all transmitting ONUs is lost. For this particular simulation, the measured wavelengths from Table 2 were uploaded to the program and the 4 upstream bonded channels were assumed with utilization of 60% to match an experiment that was performed using the setup in Fig. 12. The 60% channel utilization is equivalent to 15.6Mbps, assuming 26Mbps channel capacity. After running the simulation for a long number of data grants (100,000), the percentage of data grants lost is then calculated for each upstream channel. The simulations were run for multiple values of the minimum wavelength spacing needed to avoid OBI (e.g., 145, 165, 185 pm). In particular, the simulation uses the minimum wavelength spacing criteria in such a way that it assumes that OBI affects data grants if two wavelengths are separated by less than minimum wavelength specified in the simulation run (e.g., 145, 165, or 185pm). On the other hand, if two wavelengths are separated by more than the specified minimum wavelength separation, then no OBI is assumed. The results of the simulation are provided in Fig. 13, which show close agreement with the experimental results.

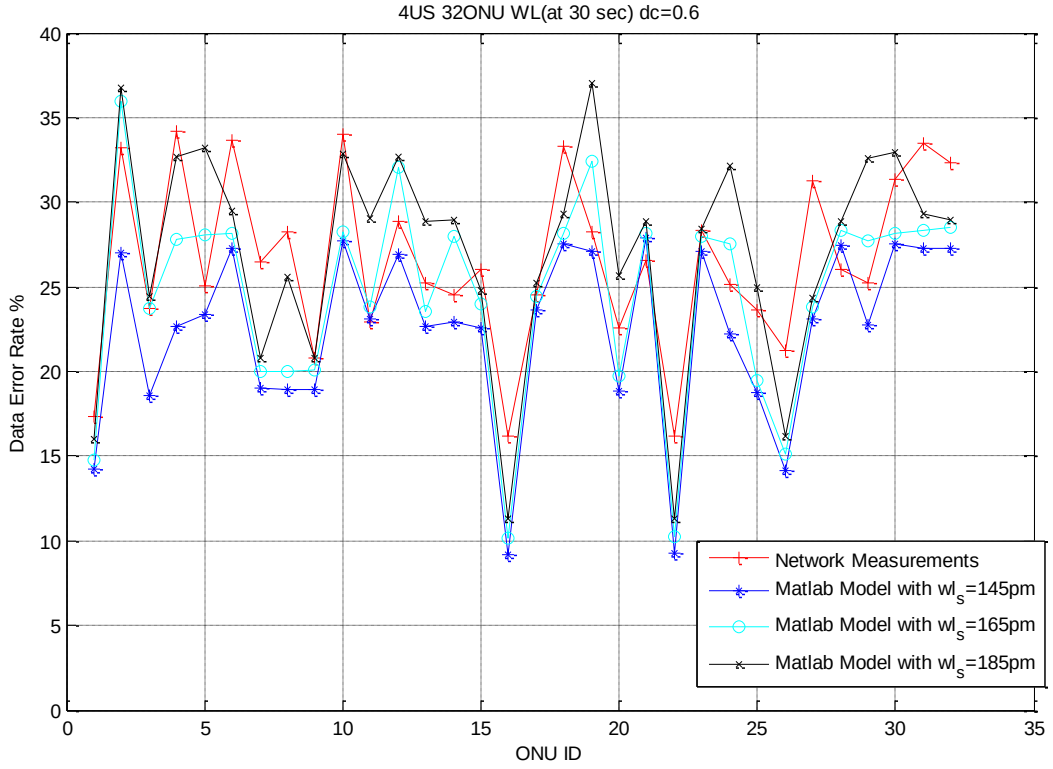


Figure 13. Data error rate measurements & simulations for a 32 RFoG ONU system

Observe that one of the specified wavelength separation values was 165 pm, which is based on a results introduced earlier in Fig. 2. Experimental results in the previous section and simulation results shown in Fig. 13 showed significant packet loss events due to the fact that ideal theoretical 165 pm value is less than the recommended 200 pm minimum separation provided earlier in this section. Moreover, the simulation environment assumed fixed wavelength values although they drift in real world.

Given that OBI can be avoided with wavelength separation values greater than 500 pm and the fact that wavelength separation

values less than 200 pm will result in significant packet loss, 200 pm-500 pm wavelength separation values will likely perform well as was shown in section 8, where some level of rare OBI events may occur due to different factors such as temperature and equipment aging.

## 10. RFOG OBI AVOIDANCE & MITIGATION

There are multiple approaches that can be taken to minimize the effect of OBI in RFoG systems. One approach is to use different wavelengths for different ONUs. While this avoids or eliminates the OBI problem overall, it is not commonly deployed and has significant cost and operations complexities. Additionally, in order to ensure that there is no OBI wavelengths must be separated from each other by at least 500 pm at all times. Since ONUs operate over a wide temperature range and the wavelength varies over temperature, it is difficult to control the wavelengths precisely enough to maintain the required separation while still fitting multiple wavelength channels into the 1610 nm window. Other methods to eliminate OBI is to allow single US transmitter at a time by either placing all ONUs on a single ATDMA US channel or scheduling a single transmitter at a time across all US channels.

Scheduler-based techniques can be developed to mitigate the effect of OBI. In particular, an OBI group/pair-aware scheduler can be designed to schedule US transmitters simultaneously such that OBI is not likely to occur based on the knowledge of the OBI groups/pairs. This will offer the most efficient and error-free network performance.

## 11. INTERACTIONS BETWEEN DOCSIS 3.1 & RFOG OBI

The introduction of DOCSIS 3.1 can extend the life of RFoG networks. This is enabled by the stretched DS & US spectra that DOCSIS3.1 devices can support. Additionally, the noise-robust OFDM PHY along with the efficient LDPC FEC technologies can support higher modulation orders to offer significant capacity increase compared to earlier DOCSIS technologies.

DOCSIS 3.1 also offers larger US channel bandwidths. In particular, US channels can be as large as 96 MHz. This can be viewed as an advantage or disadvantage depending on the OBI avoidance or mitigation scheme supported by the CMTS. For instance, if the CMTS is avoiding OBI by scheduling a single transmitter at a time across all US channels, then wide channel width will result in significant wasted capacity. When the CMTS avoids OBI by placing all CMs of an OBI group (or all CM population) on a single US channel, larger DOCSIS 3.1 channel width can be viewed as removing the capacity limitations that are introduced, when the transmitter is allowed to send traffic on a single US channel. On the other hand, if the CMTS mitigates the effect of OBI via an OBI pair/group-aware scheduler-based approach, wider channels may introduce more variables to the CMTS' scheduler as the number of CMs that can transmit at any single moment of time rises as the channel width is increased. Note that DOCSIS 3.1 can also support smaller channel widths, which can help reduce the number of potential transmitters at any instant of time.

## 12. CONCLUSIONS

This article described wavelength drift and broadening and their relation to the RFoG OBI phenomenon. Experiments and analyses showed that complete OBI-free operation requires greater than 500 pm of wavelength

separation but an acceptable network performance can be obtained with at least 200 pm of wavelength separation, which is different from the commonly accepted 20 pm recommendation for OBI-free operation. Results showed that the preamble of DOCSIS signals is robust against RFoG OBI such that the system can tolerate short transient OBI events due to fast wavelength drift. It was also shown that the OBI likelihood increases with the number of US channels. Nevertheless, solutions to mitigate and avoid RFoG OBI can be designed to offer error-free performance, where some of these solutions were demonstrated with laboratory experiments. The effect of some of the DOCSIS 3.1 features on RFoG OBI was discussed. The analysis in the paper showed that the CMTS support is critical, when a single nominal wavelength is used for US transmissions, in providing OBI-free performance in thermally-uncontrolled RFoG systems.

## REFERENCES


[1] C. Desem, "Optical Interference in Subcarrier Multiplexed Systems with Multiple Optical carriers", IEEE J on Selected Areas in Communications, Vol. 8, n. 7, Pp. 1290 – 1295, September 1990.

[2] T. H. Wolf and N. K. Shankaranarayanan, "Operation of a Passive Optical Network with Subcarrier Multiplexing in the Presence of Optical Beat Interference", IEEE JLT, Vol. 11, N. 10, Pp. 1632-1640.

[3] H. Shalom et. al., "On the Various Time Constants of Wavelength Changes of a DFB Laser Under Direct Modulation", IEEE Journal of Quantum Electronics, Vol. 34, N. 10, October 1998, Pp. 1816-1822.

[4] Calix Access Innovation, "RFoG – The advantages of an 'Intelligent' Micronode," 2009 Fiber to the Home Council Conference and Expo.

[5] Cablelabs, "Data-Over-Cable Service Interface Specifications - DOCSIS® 3.1, Physical Layer Specification, CM-SP-PHYv3.1-I02-140320," http://www.cablelabs.com/wp-content/uploads/specdocs/CM-SP-PHYv3.1-I02-140322.pdf, March 20, 2014.